

2013 Problem 15: Meniscus Optics

Optical patterns of an illuminated slit lled with liquid

ABSTRACT

The China Undergraduate Physics Tournament (CUPT) is a nationwide, annual competition for undergraduate students in China. The tournament shares the same problems and procedures with the International Young Physicists Tournament (IYPT). This paper is adapted from the solution of Peking University to Problem 15, 'Meniscus Optics', as presented in the final round of the 4th CUPT. When a slit lled with liquid is illuminated, patterns very different from the single slit diffraction pattern will appear. We carried out experiments using various light sources and measured the angular width of the fringes on a screen. We found out that the fringes can be classified into two classes, and their formations is due to geometric and wave optics domains, respectively. Based on the observations, we proposed an original model called 'the defect model' to explain the physical implications of the fringes. Numerical calculations shows that the angular width predicted by the model agrees with experiments semiquantitatively within the same scale. Other experiment phenomena can be explained using the model as well.

Keywords

Drag force, Bernoulli effect, Coandă effect, Magnus effect, Oscillation, Spin, Airstream velocity profile

Introduction

The China Undergraduate Physics Tournament (CUPT) is a nationwide, annual competition for undergraduate students in China. The tournament shares the same problems and procedures with the International Young Physicists Tournament [1] (IYPT). In each round of the CUPT three teams take turns presenting, opposing and evaluating a solution to one of the 17 problems. Here we present our solution to problem No. 15, 'Meniscus Optics', as presented in the final round of the 4th CUPT.

Heming Wang

School of Physics, Peking University, Beijing
100871, China

Yijun Jiang

Department of Physics, Massachusetts
Institute of Technology, Cambridge, MA
02139, USA

Hengyun Zhou

Department of Physics, Massachusetts
Institute of Technology, Cambridge, MA
02139, USA

Liangzhu Mu

School of Physics, Peking University, Beijing
100871, China

E-mail: muliangzhu@pku.edu.cn

When light passes a single slit, diffraction will occur and a pattern of single slit diffraction will appear on the screen with its fringes mainly extending perpendicular to the slit, and the intensity distribution is given by

$$I = I_0 \left(\frac{\sin(\alpha)}{\alpha} \right)^2, \text{ where}$$

$$\alpha = \frac{\pi a \sin \theta}{\lambda},$$

a is the width of the slit, λ is the wavelength of the incident light, and θ is the angular position of the observing point. However, if the slit is immersed in a liquid, such as water, and then removed from the liquid,

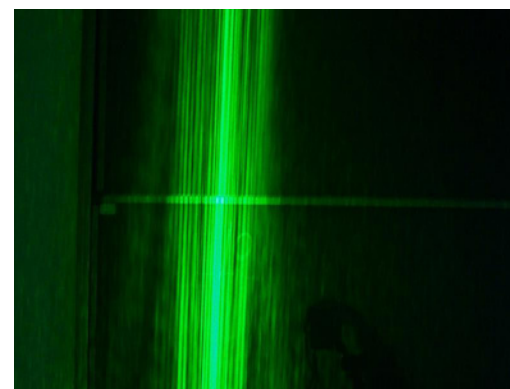


Fig. 1. Typical patterns observed in the experiments.

a liquid film is formed in the slit, and complex patterns, which are extremely different from the single slit diffraction, can be observed when this liquid slit is illuminated. A typical pattern can be seen in figure 1. The patterns extend perpendicular to the slit, but the main fringes extend along the direction of the slit. We have checked each step of our experiment carefully and believe that the pattern is resulted from the liquid-filled slit. As far as we are aware of, although relevant results on mechanical properties are present, such as the stability of liquid ridges [3] and the dynamics of menisci [4], such optical properties of liquid-filled slits have not been studied extensively in previous research.

To gain physical insight into how these fringes are generated, we carried out experiments using basic

materials and measured the angular width of the fringes. Various light sources are also used to see if different patterns can be produced. We found out that the fringes can be classified into two classes which behave differently when the width of the slit is changed or when different light sources are used. We arrived at the conclusion that the pattern is a combination of geometric optics and wave optics effects.

Then, based on our experiment results, 'the defect model' is proposed in order to explain the origin of fringes. It can be shown that more defects leads to sharper fringes, a result verified by experiments directly. In addition, numerical calculations based on this model have predicted angular widths for both classes of fringes, which agree with experiments semiquantitatively within the same scale, thus validating the model. Other experiment phenomena observed can be explained using the model and relevant optical laws as well. We believe that this can be readily applied to quick detection of defects of the μm scale.



Fig. 2. Experiment setup, which shows the semiconductor laser (bottom left), optical slit (middle) and the blackboard (right).

Experiments

2.1. Setup and procedures

The experiment is conducted in a classroom with an optical platform. We used a semiconductor laser for our light source. The power of laser is 100mW and

the wavelength is 532 nm. A standard optical slit with a variable slit width is used. Both the laser and the slit are mounted on magnetic bases with adjustable heights. In preliminary experiments, a screen is placed about 50 cm away from the slit, a normal distance in ordinary optical experiments, but the narrow fringes can hardly be distinguished. Hence in our later experiments, the blackboard, roughly 3m from the optical platform, is chosen to be the screen to receive the pattern. The whole setup is shown in figure 2.

Liquid soap is used as the liquid for the experiments, which can form a liquid film lasting hours. Its surface tension is measured to be roughly 0.3N/m. For every experiment, the slit is immersed completely in the liquid and then mounted on the base. The angle of slit is adjusted so that the incident light is normal to the slit. After a few seconds the pattern becomes stable and measurements are made on the blackboard using steel rulers.

2.2. Phenomena observed and measurements

We first conducted the experiments keeping the slit in a horizontal orientation. A typical pattern is shown in figure 1. Some very basic characteristics can be observed from the figure. The phenomenon differs greatly from the single slit diffraction pattern. This pattern extends perpendicular to the slit, diverging greatly, with divergent angle no less than 45° . Fringes appear in the direction of pattern extension.

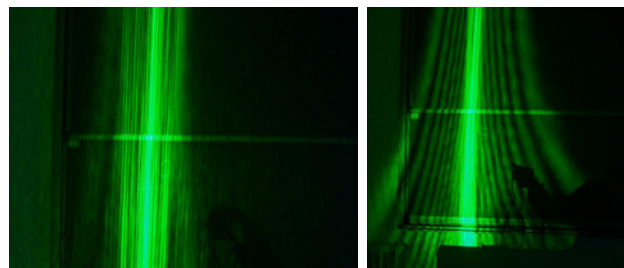


Fig. 3. Left: Typical class sides of class A fringes.

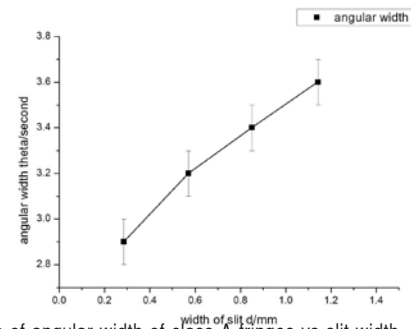


Fig. 4. Data of angular width of class A fringes vs slit width. 20 fringes are measured and averaged due to narrow fringe width and randomness of fringes.

Different patterns and fringes can be observed when we change the incident points. After many experiments, we found out that the fringes can be divided into two classes by their shape and intensity. The first kind is sharp, bright, straight and located around the center of the pattern, while the second kind is wide, faint and funnel-shaped, distributed at the sides of the pattern. For simplicity these two classes of fringes will be called class A fringes and class B fringes respectively from now on. Examples of these fringes can be seen in figure 3.

Class A fringes change slightly with different points of incidence. It is nonuniform in the horizontal direction and broadens a little at heights far away from the point of incidence. We measured the average angular width of class A fringes and found that the average angular width is positively correlated to slit width (see figure 4).

Class B fringes have distinct funnel shapes with nonuniform width at different heights. They are wider than class A fringes by an order of magnitude. They also contain the structures similar to class A fringes. The fringes differ greatly at different points of incidence, and the funnel might turn upside-down when varying the point of incidence. We also measured the angular width of class B fringes and found that the average angular width is negatively correlated to slit width, and the further the fringe is from the center, the wider it is (see figure 5).

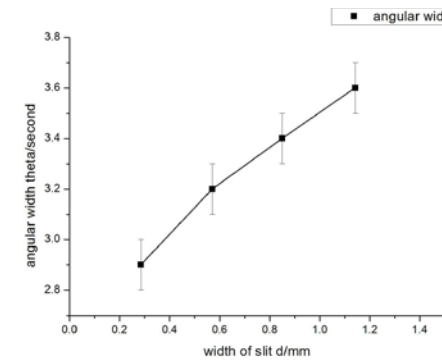


Fig. 5. Data of angular width of first 4 levels of class B fringes vs slit width. Data are measured at the same height of the slit, 3 times and averaged.

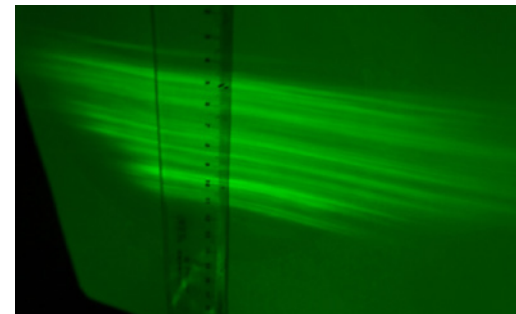


Figure 6. Fringes produced by vertically-oriented slit.

When the slit is in a vertical orientation, the pattern becomes slightly different (see figure 6). Fringes are still perpendicular to the slit, but the overall pattern is wider at the top and narrower at the bottom, due to the prominent influence of the gravity.

2.3. Effect of light sources

We also used other light sources for the experiments, including decoherented laser, ordinary white lamp light and lasers of different colors. Only class A fringe can be reproduced when laser decoherented by frosted glass or parallel white light is used. For different colors we have compared green lasers to red and blue lasers. The power of the latter two lasers are one magnitude smaller than the green laser, thus the fringes are fainter. We measured the angular width of class A fringes and found out that color does not affect the angular width. However, the low contrast of class B fringes prevented us from making comparative measurements of them.

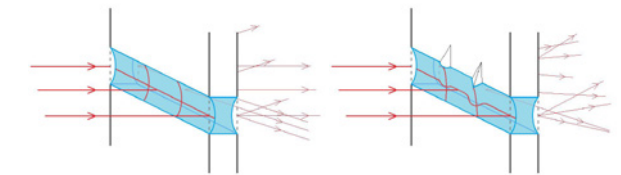


Fig. 7. Left: Illustration of a perfect slit. The light field behind the slit resembles that of a single slit diffraction field. Right: Illustration of a slit with defect. Now the light field behind the slit have random factors due to the defects.

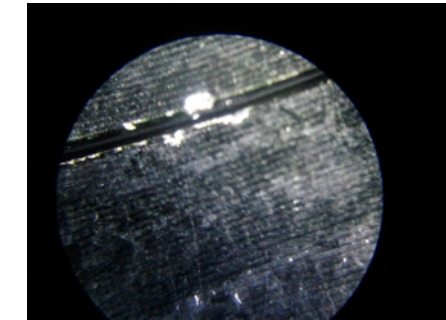


Fig. 8. Major site of defect, which produced fringes shown in figure 3b when illuminated.

Theoretical analysis

After observing the experiment phenomena, we focused on the asymmetry in the horizontal direction. If the slit is uniform in the horizontal direction, the horizontal distribution of fringes should be symmetrical, or regular at least. However, the horizontal distribution of fringes is nonuniform in the experiment, and depends on the choice of the point of incidence. After some estimations, we eliminated minor factors and identified the defects on the slit as the source of this asymmetry. Based on this consideration, we proposed a defect model to explain the phenomena observed.

The main idea of the model suggests that the slit can't be seen as a smooth rectangular hole, and defects exist along the edge (figure 7). The defects break the translational symmetry of the shape of liquid film, adding small differences at different places, causing the fringes to be nonuniform and irregular in the horizontal direction.

To confirm the validity of this model preliminarily,

we found a major site of defect, which can be observed on the slit when viewed under a position-reading microscope (see figure 8). Fringes were extremely notable when this site is chosen as the point of incidence (figure 3b), thus supporting "the defect model" vigorously.

We then focus on if the fringe formation belongs to the geometrical optics or the wave optics domain. By the results from the experiments using various light sources, it can be seen that class B fringes can only be produced by coherent light sources. On the other hand, the angular width of class A fringes are independent of the wavelength used. We therefore conclude that class A fringes is formed mainly due to simple intensity superposition (geometrical domain), and Class B fringes is formed mainly due to phase superposition (wave domain).

Comparison

Numerical calculations were made to compare our model to the experiment data. Based on different principles, we made two computer simulations. One is based on waveoptical laws corresponding to class A fringes, and the other one geometrical-optical laws corresponding to class B fringes.

To quantitatively study the impact of defect using numerical calculations, the concept of the defect level is introduced, which is defined as the mean relative deviations of the defect slit in the direction of width compared to the perfect slit. Mathematically it can be expressed as:

$$\epsilon = \frac{\int_0^L |h - h_0| dx}{h_0 \times L}$$

where h_0 is the average thickness, h is the thickness of slit at x , and L is the length of slit.

The algorithms are similar for both kinds of calculations. Random perturbations ('defect') with a

preset defect level ϵ are given to the thickness of the slit along its length. Then the slit is divided into sheets so that each sheet can be considered as a perfect one with no defect. The shape of the liquid lens can be solved from the Laplace equation with boundary conditions determined by the perturbed slit,

$$2\sigma \frac{d}{dw} \left(\frac{d^2 z / dw^2}{(1 + (dz/dw)^2)^{3/2}} \right) = \rho g$$

$$z(0) = h_0 + \Delta h$$

$$z(w_0) = h_0 + \Delta h'$$

where z is the thickness of the liquid film, w is the coordinate along the width of the slit, w_0 is the width of the slit, and h and h_0 are random perturbations satisfying the defect level definition. The slit is then illuminated with parallel monochromatic light. For wave optics, optical phases at different points on the screen are calculated and superposed to get the intensity distribution on the screen. For geometric optics, ray deflection angles on the two sides of the lens are used to characterize the intensity distribution.

Figure 9 shows the intensity distribution along the middle line on the screen, calculated using wave-optical principles and parameters measured from the experiment. It can be seen that symmetric defects lead to symmetric fringes, and asymmetric defects lead to asymmetric fringes. The higher the defect level and the more random the defect is, the more visible the fringe. Most importantly, fringes are nonuniformly distributed,

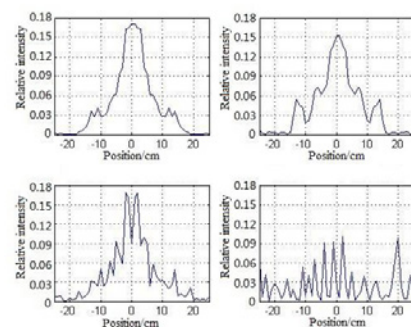


Fig. 9. Numerical calculation of wave-optical fringes. From top to bottom, left to right: No defect; Symmetric defect with $\epsilon = 0.2\%$; Random defect with $\epsilon = 0.2\%$; Random defect with $\epsilon = 0.8\%$

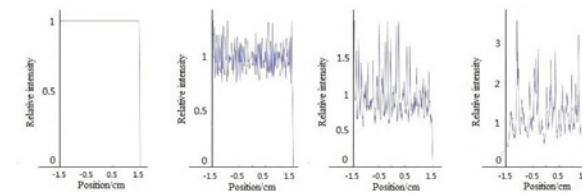


Fig. 10. Numerical calculation of geometrical-optical fringes. From left to right: No defect; Random defect with $\epsilon = 0.02\%$; Random defect with $\epsilon = 0.1\%$; Random defect with $\epsilon = 0.8\%$.

with its angular width at an order of 1×10^2 seconds, which agrees with the experiment data of class B fringes.

Figure 10 shows the intensity distribution calculated using wave-optical principles. Similar to the wave-optical case, the higher the defect level, the more visible the fringe is. Fringes have an angular width at an order of 1×10^1 seconds, which agrees with the experiment data of class A fringes.

By directly comparing figure 9 and figure 10 it can be also seen that the intensity of wave-optical fringes are much lower than geometrical-optical fringes, which agrees with the experiment as well.

This adequately demonstrates that "the defect model" and the explanations of the source of fringes based on the model are reasonable for explaining this phenomenon.

Explanation to the phenomena

We can also use our model to further explain other aspects of the phenomena qualitatively.

Average angular width of class A fringe is positively correlated to slit width A wider slit is equivalent to a lower defect level, therefore convergence and divergence centers become sparse and geometrical-optical fringes become wider.

Angular width of class B fringe is negatively correlated to slit width Wider slit width makes the liquid lens less irregular, therefore the scale of the

equivalent "optical grating" increased and wave-optical fringes become narrower.

Funnel envelopes (especially class B fringes) The equiphase surface of wavefront splitting interference is approximately a pair of hyperbolae, which diverge considerably when far away from the center.

Great divergent angle Large surface curvature near the edge will result in great deflection of the light.

Pattern of vertical-oriented slit has a wide top and a narrow bottom The pressure of the liquid at the bottom is greater than that at the top due to gravity, so the curvature is smaller. This would be equivalent to a concave lens with its (absolute value of) focal length shorter at the top, which gives a greater divergence and a wider pattern.

Discussion

We briefly studied the pattern resulting from an illuminated slit filled with liquid. Nonuniform distribution of light can be formed when a beam of light passes through a liquid-filled slit, causing fringes to appear on the screen. Fringes can be classified into two types: sharp, bright and straight class A fringes, and wide, faint and funnel-shaped class B fringes. Defects exist along the slit, causing light passing through to demonstrate geometrical and wave optical effects (class A and B fringes respectively). The defect model proposed can be used to explain experimental phenomena, and can be validated through numerical calculations. This phenomenon may find its applications in quick detection of μm scale defects.

Acknowledgments

We thank other members of the CUPT team for useful discussions. H. Wang, Y. Jiang and H. Zhou acknowledges L. Mu for providing experiment

apparatus and providing extra help.

References

- [1] IYPT, <http://www.iypt.org/Home>.
- [2] Born, M. *Principles of Optics : Electromagnetic Theory of Propagation, Interference and Diffraction of Light 7th (expanded) ed.* (Cambridge University Press, 2001).
- [3] Roy, R. V. & Schwartz, L. W. On the stability of liquid ridges. *J. Fluid Mech.* **391**, 293-318 (1999).
- [4] Clanet, C. & Quere, D. Onset of menisci. *J. Fluid Mech.* **460**, 131-149 (2002).